PERGAMON

Deep-Sea Research II 49 (2002) 3835–3848

DEEP-SEA RESEARCH
PART II

www.elsevier.com/locate/dsr2

Mesoscale distribution of dominant diatom species relative to the hydrographical field along the Antarctic Polar Front

Victor Smetacek[a,*], Christine Klaas[b], Susanne Menden-Deuer[c], Tatiana A. Rynearson[c]

[a] *Alfred-Wegener-Institute for Polar and Marine Research, Am Handelshafen 12, 27570 Bremerhaven, Germany*
[b] *Department of Geophysical Sciences, University of Chicago, 5734 South Ellis Avenue, Chicago, IL 60637, USA*
[c] *University of Washington, School of Oceanography, Box 357940, Seattle, WA 98195, USA*

Received 10 May 2001; received in revised form 18 September 2001; accepted 29 September 2001

Abstract

The quantitative distribution of dominant phytoplankton species was mapped at high spatial resolution (15 km spacing) during a quasi-synoptic, mesoscale survey of hydrographical, chemical, pigment, and zooplankton fields carried out along the Antarctic Polar Front within a grid $140 \times 130\,km^2$ during austral summer. A rapid assessment method for quantifying phytoplankton species by microscopy in concentrated samples on board enabled estimation of total biomass and that of dominant species at hourly sampling intervals. The biomass distribution pattern derived from this method was remarkably coherent and correlated very well with chlorophyll concentrations and the location of different water masses covered by the grid. A ''background'' chlorophyll concentration of $0.5\,mg\,m^{-3}$ in the grid could be assigned to the uniformly distributed pico- and nanophytoplankton; all higher values (up to $2.0\,mg\,m^{-3}$) were contributed by large diatoms. Three species complexes (*Chaetoceros atlanticus/dichaeta*, *Pseudo-nitzschia* cf. *Lineola*, and *Thalassiothrix antarctica*) contributed about one-third each to the biomass. Although all species were found throughout the study area, distinct patterns in abundance emerged: The *Thalassiothrix* maximum was located north of the frontal jet, *Chaetoceros* biomass was highest along the jet, and *Pseudo-nitzschia* was the most uniformly distributed of the three taxa. Since the meridional pattern of biomass and species composition persisted for about 5 weeks, despite heavy grazing pressure of small copepods, we hypothesize that the dominant species reflect the highest degree of grazer protection in the assemblage. This is accomplished by large size, needle-shaped cells, and long spines armed with barbs. We suggest that these persistent species sequester the limiting nutrient—iron—from the assemblage of smaller, less-defended species that must hence have higher turn-over rates.

1. Introduction

Phytoplankton of the Southern Ocean can be differentiated into two categories on the basis of size and turnover rate: the pico- and nanophytoplankton components of the ''microbial food web'' and the microphytoplankton comprised of large-celled or chain-forming diatoms and *Phaeocystis* colonies. Smetacek et al. (1990) hypothesized that spatial distribution of pico- and nanoplankton is fairly homogeneous and undergoes only moderate seasonal fluctuation in biomass in contrast to microplankton biomass, which fluctuates widely and may be responsible for all substantial

*Corresponding author.

0967-0645/02/$ - see front matter
PII: S0967-0645(02)00113-3

accumulation of biomass (blooms) above the "background level" of the microbial network. This has since been confirmed for the Weddell-Scotia Confluence (Garrison et al., 1993) and the Antarctic Circumpolar Current (ACC) (Detmer and Bathmann, 1996; Waters et al., 2000). It appears that, despite high growth rates, the biomass levels of the pico- and nanophytoplankton are constrained by high mortality rates exerted by protistan grazers. In contrast, the larger, relatively slow-growing microphytoplankton are less easily grazed and can thus accumulate biomass. It is the growth and biomass of these larger phytoplankters that contribute most to biogeochemical processes such as draw-down of CO_2 (de Baar et al., 1995) and vertical flux of biogenic elements to the ocean interior and deposition in the sediments (Smetacek, 1999).

Diatom blooms have been observed in the ACC in association with the Polar Front (APF). The phenomenon has been explained by a favourable light climate induced by shallowing of the surface mixed layer along convergent fronts (Lutjeharms et al., 1985). The availability of iron has also been shown to be a critical factor (Martin et al., 1990; de Baar et al., 1995). The build-up of phytoplankton biomass in relation to hydrography, nutrients (including iron), and grazing pressure was investigated systematically by a series of transects along the 10°W meridian during austral spring of 1992 (Smetacek et al., 1997). Three distinct blooms, dominated in each case by a single diatom species, developed in the Polar Frontal Zone during the course of a few weeks (Bathmann et al., 1997a). The comparatively rapid growth of the blooms was attributed to unusually high iron concentrations recorded in the ambient water (de Baar et al., 1995). However, since high biomass levels were also found in deeply mixed waters (Bathmann et al., 1997a), the role of hydrography in promoting biomass build-up remained obscure (Veth et al., 1997). Even more obscure were the factors determining species dominance in the three blooms.

Not much is known about the autecology of dominant ACC diatoms, although accumulation of their frustules in the underlying sediments constitutes the largest sink of biogenic silica in the ocean (Tréguer et al., 1995). Relatively few of the common ACC diatom species are represented in the underlying sediment, implying that frustules of most species dissolve in the water column. Since frustules of different species obviously have different dissolution rates, the silicon dynamics in the ACC will be governed by the species composition in the surface layer. Unfortunately, most biogeochemically oriented studies have not addressed the species level. At best, lists of the dominants are provided without attempts at interpreting their distribution patterns. However, since diatom species differ significantly in their growth requirements, behaviour, and life cycle strategies (Smetacek, 1985, Crawford, 1995) but also in properties such as Si:C:N and C:Fe ratios (Brzezinski, 1985; Timmermans et al., 2001), elucidating the underyling reasons for their occurrence will further our understanding of ocean fluxes and biogeochemistry. Verity and Smetacek (1996) have pointed out that ocean biogeochemistry is driven by comparatively few species, with the majority playing a background role. They recommend specific studies of the biology of these key functional species as a means to understand the forces shaping ecosystem structure and driving biogeochemical fluxes.

Phytoplankton biomass distribution based on pigment concentrations in the surface ocean has been recorded extensively by remote sensing, and the causative factors for the patterns are now reasonably well understood. However, comparable spatial information on distribution of individual species is lacking. Since records of phytoplankton species composition tend to be from individual water columns spaced along transects, it is not known how "species fields" relate to hydrographical and chlorophyll fields on the mesoscale (tens to hundreds of kilometres) in the open ocean, particularly within blooms. This knowledge is a prerequisite to elucidate the biology of dominant species.

To acquire this information, we assessed the spatial distribution patterns of major microplankton species at high resolution over a grid of $140 \times 130\,km^2$ in the region of the Polar Front during an R.V. *Polarstern* cruise carried out in austral summer (December 1995–January 1996).

The aim of the cruise was to examine the relationship between frontal dynamics, nutrient fields, and phyto- and zooplankton distribution, by surveying grids across the APF with a towed undulating instrument package (SeaSoar). The patterns in abundance of the dominant microplankton species in surface water were mapped during the SeaSoar surveys at sampling distances of about 15 km. Since this entailed a large number of samples, counting individual cells would have been too time-consuming. Instead a rapid method involving ranking of phytoplankton density in concentrated samples by light microscopy was developed, which enabled sample processing at hourly intervals during the surveys. The density ranks obtained on board ship were calibrated by subsequent detailed counting of individual samples in the laboratory and the results expressed in mg carbon biomass m^{-3}.

Here we present the data from the mesoscale survey and show that spatial distribution patterns of individual species matched the hydrographical field. Emboldened by this coherence, we speculate on environmental factors responsible for selecting the dominant species in the respective water masses.

2. Materials and methods

This study, entitled "Frontal dynamics and biology", was conducted in the framework of the Southern Ocean Joint Global Ocean Flux Study (SO JGOFS) and carried out in the Atlantic sector of the ACC during cruise ANT XIII/2 of R.V. *Polarstern* from 4 December 1995 to 26 January 1996. The data presented here were obtained during two quasi-synoptic SeaSoar surveys covering different scales: The coarse-scale survey (CSS) consisted of six parallel meridional sections 75 km apart and 220 km long; and the fine-scale survey (FSS), nested in the northeastern corner of the CSS, consisted of 11 meridional transects 13 km apart and 130 km long (Strass et al., 2002a, b).

The microplankton species composition and biomass contribution of dominants were assessed at hourly intervals. Surface water samples were taken with a stainless steel bucket from the moving ship. This collection method was chosen as it proved to be much less destructive for phytoplankton and protozooplankton when compared with samples taken from the different seawater pumps, which tended to break chains and even individual cells. The bucket samples were taken from mixed water from the rear of the ship and were hence representative of the upper few metres.

To obtain a sample sufficiently dense for immediate microscopic examination, the following standardized steps were taken: 3 l of bucket sample were concentrated to 50 ml by gently pouring the sample through a 20-μm mesh net cup. To facilitate rapid settling of the cells, samples were fixed with acidic Lugol's iodine solution. Three millilitres of the concentrated sample were settled in a Hydrobios sedimentation chamber and examined with a Zeiss inverted microscope at magnifications between $63\times$ and $400\times$. The rest of the sample was discoloured with a few drops of sodium thiosulfate ($Na_2S_2O_3$) and fixed with hexamine buffered formaldehyde for enumeration and calibration in the laboratory (3% final formalin concentration).

The plankton concentration in the samples obtained by our method was equivalent to settling the contents of 170 ml of seawater in the sedimentation chamber. Densities in the samples ranged from many cells or chains in close proximity to one another to only few cells in the entire chamber. To facilitate rapid analysis of each sample we developed a system by which overall microphytoplankton density was ranked highest (5) to lowest (0) at 0.5 step intervals. In addition, the density of dominant microphytoplankton species (see below) in each sample was scored as relative percentage of total microphytoplankton by estimating the percent area occupied by the species in comparison to the total plankton assemblage in the sedimentation chamber. Since six persons were involved with this subjective method of sample assessment, the ranking system was established and cross checked through simultaneous observation (by all six persons) of samples from the CSS when long meridional transects crossed from high to low biomass regions in the north and south of the investigation area. The differences in density were sufficiently large to establish general agreement on

the system of ranking. Individual results were compared regularly to ensure standardization. Each person covered about 1.5 meridional transects of the FSS.

Independent of dominance, the contribution of the following species or groups to total diatom density was assessed in each sample: *Chaetoceros atlanticus/dichaeta* species complex (termed *C. atlanticus* below), *Pseudo-nitzschia* cf. *lineola*, *Thalassiothrix antarctica* (the similar *Trichotoxon reinboldii* was also present but much less abundant), *Fragilariopsis kerguelensis*, and *Corethron criophilum*. Other diatom species were also identified and their status recorded. The apparent physiological state of the diatom population was assessed on the basis of frequency of dividing cells, incidence of plasmolysis, and presence of empty or broken frustules.

After the cruise, 14 of the concentrated and fixed plankton samples were counted in the laboratory in order to calibrate the on-board density estimates. Samples were settled in an Hydrobios chamber, and the microplankton assemblage was counted over the whole chamber with a Zeiss inverted microscope. The sizes of dominant species were measured and their volume calculated from equivalent geometrical shapes. Cell volume was converted to cellular carbon content through

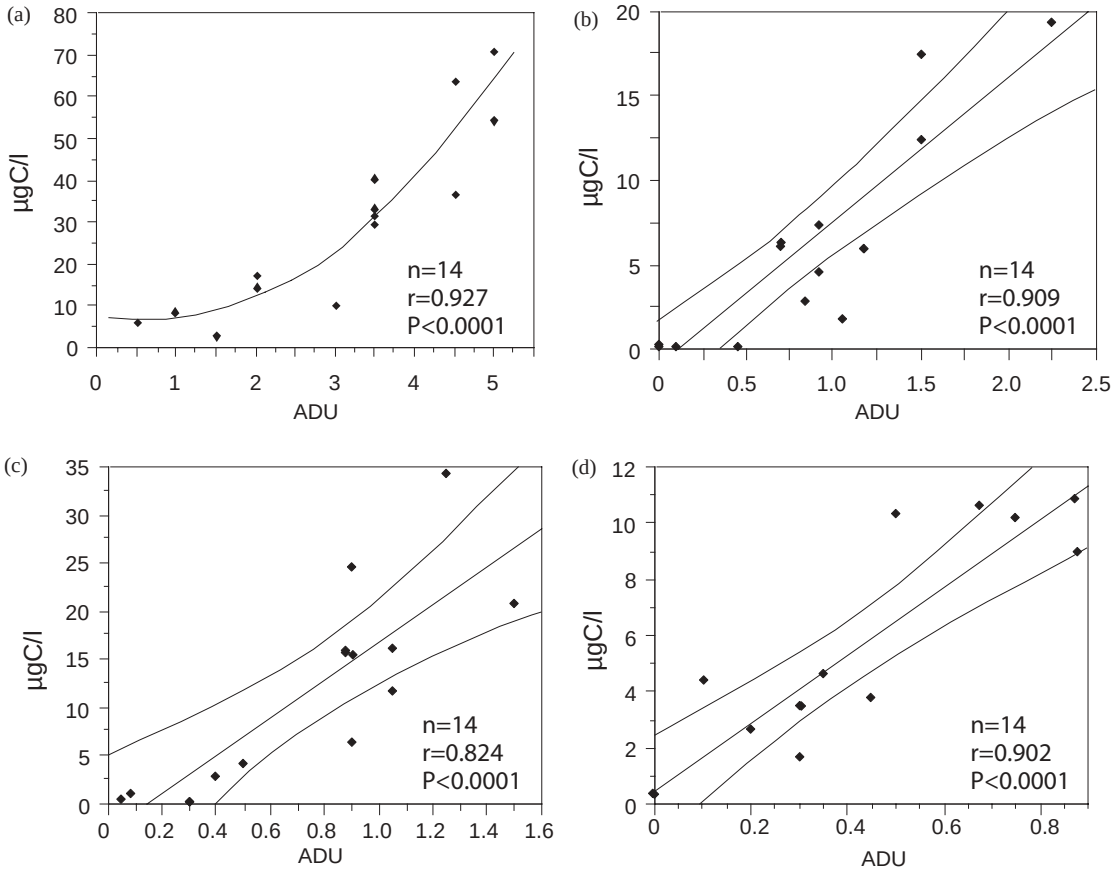

Fig. 1. Calibration curves with which total microphytoplankton density and that of dominant taxa, ranked on a scale of 0–5 in arbitrary density units (ADU), was converted to biomass (in µg $C l^{-1}$) on the basis of detailed cell counts: (a) total diatoms (> 20 µm), (b) *C. atlanticus* complex (including *C. dichaeta*), (c) *Pseudo-nitzschia* cf. *lineola*, and (d) *T. antarctica*. The calibration curves represent the best fit after comparing *F* values and residuals of different models. (*n* is the number of samples, *r* the regression coefficient and *P* is probability of density ranks; see text for more details).

recommended carbon conversion equations (Menden-Deuer and Lessard, 2000).

Regressions of the carbon biomass of the 13 samples calculated from cell counts in the laboratory with density ranks estimated on board ship yielded a highly significant relationship. In all cases the best fit was given by a polynomial relationship; however, only for the calibration of total diatom carbon standing stocks was the coefficient for the order-2 exponent significantly different from zero. For the three dominant diatom species groups, a linear calibration curve was applied whereas for the calibration of total carbon standing stocks a second-order polynomial model was used. The resulting regression equation was then applied to convert the density ranks of all samples from the FSS to estimate diatom biomass. The 14 calibrated samples also were analysed with respect to cell counts and sizes of the dominant species. The results were used to convert the density estimate for the abundant species in each sample to specific carbon biomass (Fig. 1).

3. Results

The microphytoplankton throughout the study area was dominated by *C. atlanticus*, *Pseudo-nitzschia* cf. *lineola*, and *Thalassiothrix* spp., with the former two species contributing most to the total microplankton biomass. Since many chains of the species *C. atlanticus* and *C. dichaeta* are difficult to differentiate we refer to them as the species complex *C. atlanticus* because most of the chains that could be clearly identified belonged to this species. *F. kerguelensis* and *C. criophilum* also occurred throughout but only in low numbers. Usually, both *Rhizosolenia chunii* and *R. cylindrus* contributed about 5% each to the diatom biomass. *Dactyliosolen antarcticus* was observed in all samples but never contributed significantly to the biomass. Other species present in low numbers were *Chaetoceros aequatorialis*, *C. bulbosus*, *C. convolutus*, *C. criophilus*, *C. neglectus*, *C. socialis*, *Corethron inerme*, *Eucampia* spp., *Membraneis* spp., *Pleurosigma* spp., *Pseudo-nitzschia heimii*, *Proboscia alata*, *Rhizosolenia antennata*, *Thalassiosira* spp., and *T. reinboldii*, as also various thecate and athecate dinoflagellates, foraminifera, copepods, and nauplii. *Phaeocystis* colonies attached to *Chaetoceros* chains were observed but not systematically recorded as they were generally at the four- to eight-celled stage and easily escaped detection. Their contribution to biomass was negligible throughout the ACC.

A comparison of the chlorophyll distribution recorded with a fluorometer from seawater pumped from 8 m depth in the ship's bow and calibrated at 3-h intervals (Hense, 1997) with the estimated biomass values of microphytoplankton (Fig. 2) shows a high degree of congruence both for the FSS ($C = 7.67 + 38.2 \times \text{Chl } a$, $r^2 = 0.570$, $p < 0.0001$) and the CSS ($C = -9.4 + 42.6 \times \text{Chl } a$, $r^2 = 0.688$, $p < 0.0001$).

On the basis of a three-dimensional analysis of the hydrography of the region obtained from data of the CSS and FSS, Pollard et al. (2002) differentiate three major water masses in the FSS: A tongue of colder water in the southeastern corner of the FSS originating from the southern ACC (Antarctic Zone Water, AAZ) and two broad bands of water stretching across the FSS from east to west. These bands are located on either side of the Polar Frontal jet and are termed northern and southern Polar Front Zone (NPFZ and SPFZ), respectively, by Pollard et al. (2002). The boundaries of these water masses have been indicated in Fig. 2, which depicts the distribution of total diatom carbon in the FSS. The NPFZ is characterized by high biomass ($> 40\,\text{mg C m}^{-3}$) with intermediate values in the SPFZ and very low biomass in the AAZ ($< 10\,\text{mg C m}^{-3}$).

The biomass distribution of the dominant taxa *Pseudo-nitzschia* cf. *lineola*, *C. atlanticus*, and *Thalassiothrix* spp in the FSS has been depicted in Fig. 3b–d. All three species occur throughout the FSS but *Chaetoceros* and *Thalassiothrix* are nearly absent in AAZ waters. Biomass of *Pseudo-nitzschia* is the most evenly distributed of the three species, hence is the dominant contributor to biomass at lower levels in the AAZ and parts of the SPFZ. *Chaetoceros* biomass most closely follows chlorophyll concentrations, indicating that higher values of the latter, particularly along the frontal jet, are due to this taxon. In contrast, higher concentrations of *Thalassiothrix* spp. are

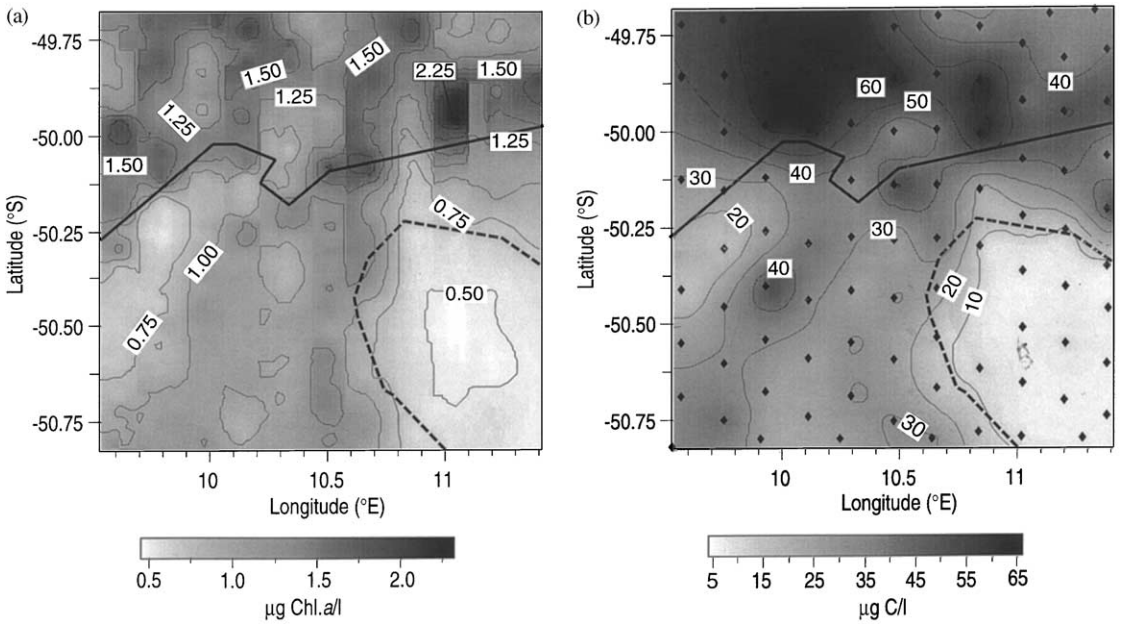

Fig. 2. Distribution of (a) chlorophyll *a* (in mg m^{-3}) based on calibrated 5-min recordings of in vivo fluorescence at 8 m depth (Hense, 1997), and (b) biomass distribution of total diatoms (> 20 µm) in units of mg carbon m^{-3} in the FSS grid. Diamonds indicate locations where phytoplankton biomass was assessed on the basis of cell counts (data in Fig. 1). The lines represent the boundaries of water masses after Pollard et al. (2002). Solid line represents the boundary between NPFZ and SPFZ. Dashed line represents the boundary between SPFZ and AAZ (Antarctic zone).

restricted to the NPFZ, along the northern rim of the FSS. Apparently, this species has its maximum north of the frontal jet, also indicated by results from the CSS, which found *Thalassiothrix* biomass values in the same range as the *Chaetoceros* maxima but some 30 km to the north of the FSS. Since only four transects were recorded in the CSS, and the species dominance patterns were similar to those recorded in the FSS, the results are not depicted here.

Despite the low silicic acid concentrations (< 6 µM) in the regions where *Thalassiothrix* was most abundant, cells of this species invariably looked healthy and no empty or broken shells of this species were found. In contrast, *Pseudo-nitzschia* chains with cells that were either empty or contained shrunken cytoplasm were often found thoughout the FSS. Such chains tended to be covered with bacteria. Generally chains with degenerated cells co-occurred with healthy chains containing many dividing cells. As these observations were not collected systematically they are not presented here in detail.

4. Discussion

The results of the rapid assessment of total microphytoplankton density correlated very well with the chlorophyll distribution. However, the latter varied by a factor of 4 across the FSS (from ca. 0.5 to 2.0 mg Chl. m^{-3}), whereas microplankton carbon varied 7-fold (from < 10 to > 60 mg C m^{-3}), with higher values corresponding well with those of chlorophyll. This indicates that variance in the chlorophyll field was mostly due to changes in the relative abundance of the microplankton, in conformity with the two-group view of phytoplankton composition proposed by Smetacek et al. (1990). It follows that a "background" chlorophyll concentration of ca. 0.5 mg m^{-3} can be assigned to the pico- and

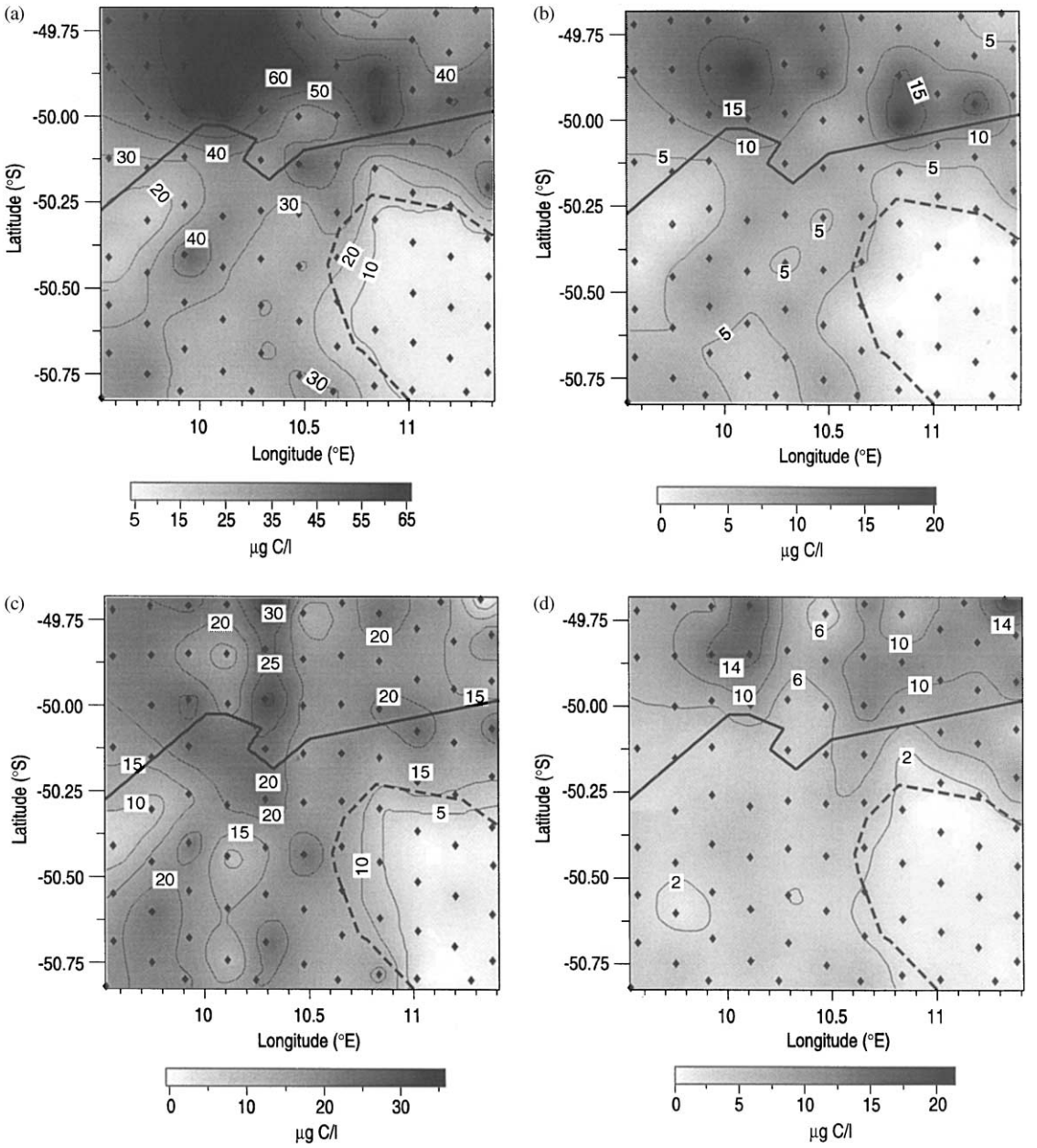

Fig. 3. Biomass distribution in mg carbon m^{-3} of (a) diatoms (>20 µm), (b) *C. atlanticus* complex (including *C. dichaeta*), (c) *Pseudonitzschia* cf. *Lineola*, and (d) *T. antarctica* in the FSS. Note different scales in all four panels. Lines as in Fig. 2.

nanophytoplankton of the microbial network in this season and that values above this level are contributed by microphytoplankton.

Chlorophyll measurements on size-fractionated samples from individual stations in the investigation area carried out by Tremblay et al. (2002) confirm this conclusion. The average microphytoplankton carbon:total chlorophyll ratio in the FSS was 38. If the contribution of the microbial chlorophyll is added, the ratio increases to about

50, which lies well within the range of empirically measured values reported in the literature. The fact that chlorophyll distribution (recorded at 5-min, i.e. 1.2-km intervals) more or less matches that of diatom carbon (recorded at hourly, i.e. 15-km intervals) indicates spatial homogeneity of species fields over tens of kilometres within water masses, accompanied by sharp demarcations between them. It follows that similar hydrographical conditions give rise to similar species assemblages and abundances.

Vertical profiles of species abundance and compositon from discrete water samples collected along a transect through the centre of the FSS after its completion showed that biomass of the different species was generally distributed homogeneously through the water column (Schülke, 1998). An exception was found in the *Thalassiothrix* population in the silica-exhausted water along the northern boundary of the FSS. At some stations in this region, the surface concentrations of this species were about half those in the lower part of the mixed layer. With these exceptions, the surface samples analysed during the surveys can be considered as representative of the mixed layer.

The coherence of our phytoplankton biomass values with the other parameters measured invites further interpretation. The species we encountered are typical of the region and season, but the fact that their respective biomass distributions exhibited intriguing similarities and differences encourages interpretation of the possible underlying causes.

4.1. Physical environment

The biomass of large diatoms and chlorophyll concentrations correspond remarkably well with the different water masses encountered in the FSS, indicating that hydrography is the primary determinant of phytoplankton abundance and species composition. Interpreting the low biomass in the colder water of the AAZ and the higher biomass in the warmer water of the NPFZ as a temperature effect is not justified, as the temperature range across the water masses was only 1.2°C (ranging from <3.4 to >4.6°C). Rather, the dynamics and hence history of the water masses are likely to have played the decisive role.

Strass et al. (2002a) analysed the mesoscale frontal dynamics of the region in terms of its influence on primary production. They showed that the FSS covered a meander structure of the Polar Front and a cold cyclonic eddy located to its southeast—the AAZ. Because of the north–south density gradient, there is a tendency for northern, lighter water to overlie water from the south. The dynamics of this cross-frontal circulation results in patchy distribution of shallow and deep mixed layers on horizontal scales of tens to hundreds of kilometres and time scales of days to weeks. The degree of patchiness increases along the southern flank of the meander, i.e. in the SPFZ and is reflected in the tongues of lower and higher biomass that extend from southwest to northeast in the FSS. In contrast the NPFZ and the AAZ exhibit much less spatial heterogeneity.

It follows that the phytoplankton populations in the SPFZ region will have experienced considerable spatial and temporal fluctuation in light climate. Portions of the population will have been favoured by shallow (<40 m) mixed layer depths for a week or so whereas others will have been mixed or downwelled to unfavourable depths (>60 m). The situation for a given population could have been reversed some days or weeks later. This fluctuating scenario is supported by the results obtained from a series of stations occupied along a transect through the centre of the FSS following its completion (Hense, 1997; Schülke, 1998). These studies reported 2-fold differences in mixed-layer depths of water columns 10 km apart. Although shallow mixed layers generally carried higher phytoplankton biomass, particularly in the NPFZ, exceptions were found where biomass was low in shallow mixed depths. Presumably the latter was recently formed and the diatoms had not had time to respond. In conclusion, frontal dynamics subject phytoplankton to a range of growth environments at time scales of about a week—the average period between storms. This type of "habitat patchiness" is higher along the southern flank of the front and contrasts with the uniform deep mixed layers and low biomass of the AAZ south of the front. Fluctuating vs. stable growth

environments could well favour different types of growth strategies in the phytoplankton discussed below.

4.2. Chemical environment

Macronutrient concentrations also reflected the position of the three zones very accurately. The patterns of nitrate and silicic acid showed similar spatial trends, whereas nitrate ranged from 20 to 25 mmol m^{-3} from the AAZ to the NPFZ, silicic acid exhibited a much stronger gradient: 2–26 mmol m^{-3}, respectively (Bathmann et al., 1997b). Thus, silicic acid was at limiting concentrations for the diatoms in the northern fringe of the FSS. Since the maximum of the *Thalassiothrix* population was located in the lower half of the mixed layer at some stations in the NPFZ (Schülke, 1998), it seems likely that this was due to gradual sinking out of a part of the Si-limited population from the upper mixed layer. Schülke (1998) estimated that the bulk of the biogenic silica present in the water column was in *Thalassiothrix* frustules, indicating that this population had extracted Si down to limiting levels for net diatom growth prior to our measurements.

Concentrations of dissolved iron, measured continuously during the grid from an independent uptake system, were uniformly low (0.15–0.45 nM) throughout the study area and showed no tendency to correlate with any of the parameters measured on the cruise (de Jong et al., 1998). However, this does not mean that the biomass distribution we found was not a reflection of past iron availability. Since we could not ascertain any significant temporal trend in the values we found in the region of the FSS over the 5 weeks of investigation, it seemed that little, if any, biomass accumulation was occurring at the time, although net primary production was substantial (see below). Hence one might postulate that iron concentrations behaved in a fashion similar to silicic acid, i.e. they had been higher prior to our arrival in the NPFZ, and that this "excess" iron had been incorporated into the higher biomass we encountered. A part of this iron would be undergoing regeneration by heterotrophs in the heavily grazed microbial food web but also incorporated in the unusually high copepod standing stocks that occurred throughout the area (Pollard et al., 2002). This hypothesis is developed further below.

4.3. Biological environment

The results of an optical plankton counter mounted on the SeaSoar, calibrated by net samples from a series of stations, showed the biomass of mixed small copepods and their juvenile stages in the PFZ was in the same range as that of the phytoplankton—ca. 6 g C m^{-2}—calculated on the basis of a carbon:chlorophyll ratio of 50 (Pollard et al., 2002). This unusually high copepod biomass will have exerted considerable feeding pressure on the pelagic system, although we can only conjecture as to how this will have contributed to structuring it.

Small copepods are known to be selective feeders that collect and ingest their food item by item. They are reported to prefer mobile prey such as ciliates and heterotrophic dinoflagellates (Kleppel et al., 1991; Atkinson, 1996) but also ingest faecal pellets (González and Smetacek, 1994) and diatom chains that they crush with their mandibles. Thus, they break off the siliceous spines of *Chaetoceros* cells and ingest the chains. However, there will be an upper limit to the size of cells a copepod can handle. Since the chains of the *C. atlanticus* complex are very large (the spines are several 100 μm across) and *Thalassiothrix* cells are up to 5 mm long, these taxa are in the same size range as the small copepods and copepodites. Since no damaged cells or pieces of frustule of these species were found, although looked for, we suggest that these large diatoms were not grazed by the smaller copepods and thus accumulated in the water column. In contrast, the *Pseudo-nitzschia* species were small enough to be grazed, although we do not know to what extent. The chains of this species tended to be very long, (>30 cells), indicating that they were several weeks old or had higher growth rates than the other dominant species.

The fact that, by and large, the distribution of copepods coincided with that of the large diatoms (Pollard et al., 2002) is an indication that these were not their preferred food item, as they would

not have accumulated otherwise. On the basis of a diagnostic model of primary production mapped on the hydrographical field of the FSS, Strass et al. (2002a, b) calculated integrated primary production in the order of 0.3–1.0 g $C\,m^{-2}\,d^{-1}$, with higher values corresponding with biomass. Tremblay et al. (2002) measured primary production in water columns selected for areal coverage throughout the 5 weeks of the cruise. They commented that a net increase in biomass in the investigation region was not evident, indicating that daily primary production was being utilized at high efficiency. Dubischar et al. (2002) reported that, despite the high copepod stocks, faecal pellets were present in conspicuously low numbers, also suggesting efficient reworking of organic matter other than that of the large diatoms. Smaller diatoms, including various *Chaetoceros* species, were ubiquitous but dwarfed by the dominant diatoms. The former are likely to have been dividing at faster rates than larger species but since they did not accumulate biomass, they must have concomitantly suffered higher loss rates.

4.4. Distribution of dominant species groups

The biomass distribution patterns of the three dominant species groups reflected the hydrographical field over the breadth of 225 km covered by the CSS. The spatial coherence of species abundance within water masses is remarkable. All three species or groups were present in almost all the samples of the FSS, with low numbers in the AAZ water in the southeastern corner indicating prevalence of a potential seeding stock throughout the area. Yet differences in abundance pattern within this species assemblage suggest a temporal shift in dominance status. Whereas *Pseudo-nitzschia* and *Chaetoceros* biomass reflected the chlorophyll field, higher *Thalassiothrix* biomass occurred only north of the frontal jet. Hence the higher biomass in the NPFZ was primarily due to this latter species. This water also had the lowest silicic acid concentrations, indicating that it had the longest growth history.

Pseudo-nitzschia spp. was the most uniformly distributed of the three species groups and seemed to suffer the highest mortality rates. Chains with moribund cells, often covered with bacteria, were found only in this group. Generally all the cells of the chain were affected. Whether this signified an end of the growth phase by apoptosis or was due to infection by pathogens (bacteria or viruses) cannot be determined. Interestingly, chains with healthy dividing cells co-occurred with chains consisting of moribund cells. Since the other plankton species did not exhibit this co-occurrence of healthy and "sick" cells, it is unlikely that these had experienced very different growth conditions in the recent past and been mixed together shortly before sampling. Hence the infection explanation seems more likely. However, since the various species of *Pseudo-nitzschia* are very difficult to differentiate by light microscopy, we could have been witnessing a species succession forced by a species-specific pathogen. These speculations are meant to draw attention to possible factors driving species succession that need to be investigated.

The assemblage we encountered represents giant, spiny plankton. The cells of the *C. atlanticus* complex are up to 45 μm across and carry chloroplast-containing spines 1–2 μm thick and up to several hundred microns long. *Thalassiothrix antarctica* (the dominant species of *Thalassiothrix* observed) is also the largest and most robust species of its genus. The cells can be up to 5 mm long although they are only about 1.5–6 μm wide. The silica cell walls are themselves about 1 μm thick. The genus *Pseudo-nitzschia* combines a number of species, all with much thinner frustules than the former genera, and difficult to differentiate under the light microscope. Several species, including *P. lineola*, that seemed to dominate in the FSS, are cosmopolitan. Individual cells are 56–112 μm long and 1.8–2.7 μm wide. The tips of the cells are attached to one another forming chains of several millimetres long. The data in this paragraph are from Hasle and Syvertsen (1996).

The needle-like cells of *Pseudo-nitzschia* and *Thalassiothrix*, and the long, hollow spines filled with chloroplasts of the *Chaetoceros* complex, can be interpreted as adaptations to increase the surface:volume ratio and hence enhance nutrient uptake rates, in this case, iron. It has been suggested that long chains and cells could experience enhanced nutrient fluxes due to turbulence

compared to shorter chains and cells (Karp-Boss et al., 1966; Pahlow et al., 1997). However, the increase in uptake rates by the former is only marginal. Further, Timmermans et al. (2001) have shown that the small-celled Antarctic *Chaetoceros brevis* can grow at much lower iron levels than the very much larger, chain-forming *C. dichaeta*, which belongs to the *C. atlanticus* complex. In any case, the minute cells of the microbial network had much higher growth and hence uptake rates than the large diatoms. The fact that the needle-shaped diatoms accumulated 3 times as much biomass as the microbial phytoplankton and all the other diatoms combined can only be explained by their lower loss rates. Hence the convergence in form to long, thin needles amongst larger diatoms may well have evolved as a mechanism to deter grazing; an explanation we favour here. As mentioned above, grazing pressure by the grazer community, in particular small copepods, will have been very high, in the same range as the daily primary production (Tremblay et al., 2002).

Predator defence mechanisms in the plankton have received comparatively little attention so far but are likely to be much more widespread than currently assumed (Verity and Smetacek, 1996; Smetacek, 2001a). Both the *Chaetoceros* spines and the *Thalassiothrix* cells carry well-developed barbs that most likely serve a common function. We speculate that they provide protection from metazoan grazers (copepods and salps) as the cells will be more difficult to handle than smooth ones. In contrast, the smooth, thin-walled chains of *Pseudo-nitzschia* are delicate in comparison to the other dominants, but superficially the chains resemble the robust, long cells of *Thalassiothrix*. Whether the superficial resemblance is of significance (mimicry) needs to be studied, but if large size and spines confer protection against ingesting protists and smaller metazoan grazers, then this assemblage can be considered as well defended. It should be mentioned that parasitoids—small protists that feed on diatom plasma by inserting themselves or a feeding tube through the frustule (Kühn, 1995)—although specifically looked for, were not found.

We suggest the following scenario to explain our findings. The uniformly low iron concentrations indicate that this was the limiting nutrient throughout the FSS. The iron fuelling the high primary production levels is most likely to have emanated from regenerated sources (Barbeau et al., 1996; Barbeau and Moffett, 2000) since high phytoplankton biomass correlated with that of small copepods (Pollard et al., 2002). Under such conditions slow-growing, long-lived phytoplankton will be accumulating biomass by taking up and sequestering nutrients from the regenerating pool. Only large, strong grazers such as euphausiids will be capable of handling and crushing the needle-shaped diatoms, but they were patchily distributed and not present in large numbers (Pollard et al., 2002). Dinoflagellates that feed on diatom chains by engulfing them with a pallium (feeding veil), such as the genus *Protoperidinium*, were present but in low numbers. Since they are selectively grazed by copepods (Kleppel et al., 1991; Atkinson, 1996), their grazing pressure is likely to have been low. However, although chains of smaller *Chaetoceros* species can be handled by a single dinoflagellate (Jacobson and Anderson, 1986), it is probable that very long diatom cells and chains will pose a problem also for these grazers. Buoyancy regulation by the large diatoms is a prerequisite to permit suspension over long periods. Although the mechanisms are still poorly understood, there is little doubt that diatoms can indeed maintain their position in the surface layer (Waite et al., 1997; Waite and Nodder, 2001).

4.5. Comparison with other findings

The conditions encountered during our cruise in austral summer of 1995/1996 (ANT XIII/2) differed significantly from those reported during the spring of 1992 (ANT X/6). Iron concentrations during the latter cruise were exceptionally high in PFZ waters (de Baar et al., 1995), we believe that the iron is most likely to have been released from the many icebergs (5–15/100 km^2) present throughout the cruise across the entire ACC (van Franeker in Bathmann et al., 1994). The high iron values in the PFZ are likely to have been due to increased iceberg melt in the warmer water (2°–4°C) as opposed to the much colder AAZ south of the front (<0°C), where iron concentrations were

much lower. Quéguiner et al. (1997) reported exceptionally high loads of suspended lithogenic matter in the PFZ, which we interpret as "fossil" dust released from the melting icebergs, which were also the source of the iron. During the summer cruise in 1995/1996 not a single ice berg was observed in the ACC and iron values were uniformly low throughout (de Jong et al., 1998).

During ANT X/6 a series of diatom blooms, dominated successively from south to north by *Fragiliariopsis kerguelensis*, *C. inerme*, and *Corethron criophilum* (now *pennatum*, Crawford et al., 1998) extended from 50°S (the boundary between the PFZ and the AAZ) to 46°S (Bathmann et al., 1997a). These species, although present throughout the FSS, occurred only in low numbers during ANT XIII/2. The shapes of these diatoms are very different to the "needle plankton": the *Corethron* species are cylindrical with comparatively large vacuoles. *C. pennatum* is solitary and carries barbed spines more formidable than those of *C. atlanticus*, whereas *F. kerguelensis* is boat-shaped and, like *Thalassiothrix*, has very thick frustules. In the growth phase the chains of *F. kerguelensis* can be very long. This species also dominated the bloom stimulated by iron fertilization during the SOIREE experiment (Boyd et al., 2000), suggesting that it takes advantage of iron input to a greater extent than the other species. Smetacek (1999) has argued that its thick frustules, which are very prominent in the ACC sediments, also provide protection against grazing. However, it should be mentioned that grazing pressure in the *F. kerguelensis* blooms both during ANT X/6 and SOIREE was low.

We can conclude that the spring assemblages of 1992 were characterized by species that, under high iron availability and low grazing pressure, built up high biomass concentrations within a few weeks (ca. twice as high as recorded in the summer of 1995/1996) also in deep mixed layers. In contrast, the summer assemblage of 1995/1996 built-up biomass under low iron availability and heavy grazing pressure. Since biomass and production did not change significantly over several weeks, in contrast to the spring blooms, we suggest that these species, particularly the *C. atlanticus* complex and *T. antarctica*, tend to persist for long periods in the surface layer because of their low mortality rates. Whatever the cause of their demise, a part of their remains will eventually sink out of the surface layer. *Chaetoceros* and *Pseudo-nitzschia* frustules are rare to absent in the underlying sediment, suggesting that these genera contribute to maintaining the high silicic acid concentrations in the sub-surface water column. Zielinski and Gersonde (1997) report occurrence of *Thalassiothrix* frustules in sediments underlying the Polar Front but their absence further south, suggesting that the distribution pattern reported here is reflected in the sediment.

Kemp et al. (2000) proposed that two types of diatom assemblages are represented in the sediments: the fast-growing, relatively small-celled spring species that sediment out before the onset of summer, and the slow-growing, large-celled diatoms that sink out at the end of the summer. They refer to the latter as the "fall dump" of giant diatoms and include *Thalassiothrix* in the latter group. They suggest that this species is part of a "shade flora" that accumulates biomass at the bottom of the euphotic layer where nutrient concentrations are likely to be higher than in the overlying layer. We propose an alternative hypothesis in which this genus, because of superior grazer protection, builds up biomass by sequestering nutrients, in this case iron and silicic acid, from the regenerating pool. Testing these hypotheses with, e.g. in situ iron fertilization experiments (Boyd et al., 2000; Smetacek, 2001b), will provide information on the biology of such key species and improve our ability to reconstruct past climate conditions on the basis of the species composition of the sediments.

Acknowledgements

Stefanie Kühn and Maret Nacken were part of the team estimating phytoplankton species densities during the cruise and we thank them for their dedicated efforts. We are grateful to the captain and crew of R.V. *Polarstern* for their assistance during the cruise. Partial support for SMD was provided by Deutscher Akademischer Austausch Dienst (DAAD).

References

Atkinson, A., 1996. Subantarctic copepods in an oceanic, low chlorophyll environment: ciliate predation, food selectivity and impact on prey populations. Marine Ecology Progress Series 130, 85–96.

Barbeau, K., Moffett, J.W., 2000. Laboratory and field studies of colloidal iron oxide dissolution as mediated by phagotrophy and photolysis. Limnology and Oceanography 45, 827–835.

Barbeau, K., Moffett, J.W., Caron, D.A., Croot, P.L., Erdner, D.L., 1996. Role of protozoan grazing in relieving iron limitation of phytoplankton. Nature 380, 61–64.

Bathmann, U.V., Smetacek, V., de Baar, H.J.W., Fahrbach, E., Krause, G., 1994. The expeditions ANTARKTIS X/6-8 of the Research Vessel "POLARSTERN" in 1992/1993. Reports on Polar Research, 135, 126pp.

Bathmann, U.V., Scharek, R., Klaas, C., Dubischar, C.D., Smetacek, V., 1997a. Spring development of phytoplankton biomass and composition in major water masses of the Atlantic Sector of the Southern Ocean. Deep-Sea Research II 44, 51–67.

Bathmann, U., Lucas, M., Smetacek, V., 1997b. The expeditions ANTARKTIS XIII/1-2 of the Research Vessel "POLARSTERN" in 1995/96. Reports on Polar Research, 221, 136pp.

Boyd, P.W., 2000. A mesoscale phytoplankton bloom in the polar Southern Ocean stimulated by iron fertilization. Nature 407, 695–702.

Brzezinski, M.A., 1985. The Si:C:N ratio of marine diatoms: interspecific variability and the effect of some environmental variables. Journal of Phycology 21, 347–357.

Crawford, R.M., 1995. The role of sex in the sedimentation of a marine diatom bloom. Limnology and Oceanography 40, 200–204.

Crawford, R.M., Hinz, F., Honeywill, C., 1998. Three species of the diatom genus *Corethron* CASTRACANE: structure, distribution and taxonomy. Diatom Research 13, 1–28.

De Baar, H.J.W, de Jong, J.T.M., Bakker, D.C.E., Löscher, B.M., Veth, C., Bathmann, U.V., Smetacek, V., 1995. Importance of iron for plankton blooms and carbon dioxide drawdown in the Southern Ocean. Nature 373, 412–415.

Detmer, A.E., Bathmann, U.V., 1996. Distribution patterns of autotrophic pico- and nanoplankton and their relative contribution to algal biomass during spring in the Atlantic Sector of the Southern Ocean. Deep-Sea Research II 44, 299–320.

Dubischar, C.D., Lopes, R.M., Bathmann, U.V., 2002. High summer abundances of small pelagic copepods at the Antarctic Polar Front—implications for ecosystem dynamics. Deep-Sea Research II 49 (17), 3871–3887.

Garrison, D.L., Buck, K.R., Gowing, M.M., 1993. Winter plankton assemblages in the ice-edge zone of the Weddell and Scotia Seas: composition, biomass and spatial distribution. Deep-Sea Research I 40, 311–338.

González, H.E., Smetacek, V., 1994. The possible role of the cyclopoid copepod *Oithona* in retarding vertical flux of zooplankton faecal material. Marine Ecology Progress Series 113, 233–246.

Hasle, G.R., Syvertsen, E.E., 1996. Marine diatoms. In: Tomas, C.R. (Ed.), Identifying Marine Diatoms and Dinoflagellates. Academic Press, New York, 598pp.

Hense, I., 1997. Chlorophyllverteilung und Phytoplanktonbiomasse in der antarktischen Polarfront. Diplomarbeit, University of Bremen, Bremen.

Jacobson, D.M., Anderson, J.M., 1986. Thecate heterotrophic dinoflagellate feeding behaviour and mechanisms. Journal of Phycology 22, 249–258.

de Jong, J.T.M., den Das, J., Bathmann, U.V., Stoll, M.H.C., Kattner, G., Nolting, R.F., de Baar, H.J.W., 1998. Dissolved iron at subnanomolar levels in the Southern Ocean as determined by ship-board analysis. Analytica Chimica Acta 377, 113–124.

Karp-Boss, L., Boss, E., Jumars, P.A., 1966. Nutrient fluxes to planktonic osmotrophs in the presence of fluid motion. Oceanography and Marine Biology an Annual Review 34, 71–107.

Kemp, A.E.S., Pike, J., Pearce, R.B., Lange, C.B., 2000. The "Fall dump"—a new perspective on the role of a "shade flora" in the annual cycle of diatom production and export flux. Deep-Sea Research II 47, 2129–2154.

Kleppel, G.S., Holliday, D.V., Piper, R.E., 1991. Trophic interactions between copepods and microzooplankton: a question about the role of diatoms. Limnology and Oceanography 36, 172–178.

Këhn, S., 1995. Infection of marine diatoms by parasitoid protists. Ph.D. thesis, University of Bremen, Bremen, 150pp.

Lutjeharms, J.R.E., Walters, N.M., Allanson, B.R., 1985. Oceanic frontal systems and biological enhancement. In: Siegfried, W.R., Condy, P.R., Laws, R.M. (Eds.), Antarctic Nutrient Cycles and Food Webs. Springer, Berlin, pp. 11–21.

Martin, J.H., Fitzwater, S.E., Gordon, R.M., 1990. Iron deficiency limits phytoplankton growth in antarctic waters. Global Biogeochemical Cycles 4, 5–12.

Menden-Deuer, S., Lessard, E.J., 2000. Carbon to volume relationships for dinoflagellates, diatoms, and other protist plankton. Limnology and Oceanography 45, 569–579.

Pahlow, M., Riebesell, U., Wolf-Gladrow, D.A., 1997. Impact of cell shape and chain formation on nutrient acquisition by marine diatoms. Limnology and Oceanography 42, 1660–1672.

Pollard, R.T., Bathmann, U.V., Dubischar, C., Read, J.F., Lucas, M., 2002. Zooplankton distribution and behaviour in the Southern Ocean from surveys with a towed Optical Plankton Counter. Deep-Sea Research II 49 (17), 3889–3915.

Quéguiner, B., Tréguer, P., Peeken, I., Scharek, R., 1997. Biogeochemical dynamics and the silicon cycle in the Atlantic sector of the Southern Ocean during austral spring 1992. Deep-Sea Research II 44, 69–90.

Schülke, M. 1998. Diatomeenverteilung und—biomasse im Bereich der antarktischen Polarfront. Diplomarbeit, University of Bremen, Bremen, 65pp.

Smetacek, V.S., 1985. Role of sinking in diatom life-history cycles: ecological, evolutionary and geological significance. Marine Biology 84, 239–251.

Smetacek, V., 1999. Diatoms and the ocean carbon cycle. Protist 150, 25–32.

Smetacek, V., 2001a. A watery arms race. Nature 411, 745.

Smetacek, V., 2001b. The greening of a Southern Ocean eddy. Weekly reports from the chief scientist on the EisenEx cruise. Ocean Challenge 10, 21–74526.

Smetacek, V., Scharek, R., Nöthig, E.-M., 1990. Seasonal and regional variation in the pelagial and its relationship to the life history cycle of krill. In: Kerry, K.R., Hempel, G. (Eds.), Antarctic Ecosystems: Ecological Change and Conservation. Springer, Berlin, pp. 103–114.

Smetacek, V., de Baar, H.J.W., Bathmann, U.V., Lochte, K., Rutgers van der Loeff, M.M., 1997. Ecology and biogeochemistry of the Antarctic Circumpolar Current during austral spring: a summary of Southern Ocean JGOFS cruise ANT X/6 of RV Polarstern. Deep-Sea Research II 44, 1–21.

Strass, V.H., Naveira Garabato, A.C., Pollard, R.T., Fischer, H.I., Hense, I., Allen, J.T., Read, J.F., Leach, H., Smetacek, V., 2002a. Mesoscale frontal dynamics: shaping the environment of primary production in the Antarctic Circumpolar Current. Deep-Sea Research II 49 (17), 3735–3769.

Strass, V.H., Naveira Garabato, A.C., Bracher, A.U., Pollard, R.T., Lucas, M.I., 2002b. A 3-d mesoscale map of primary production at the Antarctic Polar Front: results of a diagnostic model. Deep-Sea Research II 49 (17), 3813–3834.

Timmermans, K.R., Gerringa, L.J.A., de Baar, H.J.W., van der Wagt, B., Veldhuis, M.J.W., de Jong, J.T.M., Croot, P.L., Boye, M., 2001. Growth rates of large and small Southern Ocean diatoms in relation to availability of iron in natural seawater. Limnology and Oceanography 46, 260–266.

Tréguer, P., Nelson, D.M., Van Bennekom, A.J., DeMaster, D.J., Leynaert, A., Quéguiner, B., 1995. The silica balance in the world ocean: a reestimate. Science 268, 375–379.

Tremblay, J.E., Lucas, M.I., Kattner, G., Pollard, R., Strass, V.H., Bathmann, U.V., 2002. Significance of the Polar Frontal Zone for large-sized diatoms and new production during summer in the Atlantic sector of the Southern Ocean. Deep-Sea Research II 49 (17), 3793–3811.

Verity, P., Smetacek, V., 1996. Organism life cycles, predation, and the structure of marine pelagic ecosystems. Marine Ecology Progress Series 130, 277–293.

Veth, C., Peeken, I., Scharek, R., 1997. Physical anatomy of fronts and surface waters in the ACC near the 6°W meridian during austral spring 1992. Deep-Sea Research II 44, 23–50.

Waite, A., Nodder, S.D., 2001. The effect of in situ iron addition on the sinking rates and export flux of Southern Ocean diatoms. Deep-Sea Research II 48, 2635–2654.

Waite, A., Fisher, A., Thompson, P.A., Harrison, P.J., 1997. Sinking rate vs. volume relationships illuminate sinking control mechanisms in marine diatoms. Marine Ecology Progress Series 157, 97–108.

Waters, R.L., van den Enden, R., Marchant, H.J., 2000. Summer microbial ecology off East Antarctica (80–150°E): protistan community structure and bacterial abundance. Deep-Sea Research II 47, 2401–2435.

Zielinski, U., Gersonde, R., 1997. Diatom distribution in southern ocean surface sediments (Atlantic sector): implications for paleoenvironmental reconstructions. Palaeogeography, Palaeoclimatology, Palaeoecology 129, 213–250.